Development of On-line Optimization-Based Control Strategies for a Starved-Feed Semi-batch Copolymerization Reactor

Onyinye E Okorafo, Luis Fernando Torres, Robin A Hutchinson and Martin Guay. Chemical Engineering, Queen's University, 19 Division St, Dupuis Hall, Kingston, ON K7L 3N6, Canada.

Introduction

Acrylic resins for automotive coatings are of great interest to the polymer industry. Most automotive coating resins are complex copolymers primarily composed of styrene, acrylate, and methacrylate monomers. A "starved-feed" feeding policy is implemented that involves adding the initiator and monomer to the reactor at a constant rate over several hours. This feeding strategy is employed at high temperature conditions to ensure uniform average molecular weight and copolymer composition while operating at relatively low solvent levels. At these conditions of low monomer concentrations, high instantaneous conversion is achieved which results in polymer with relatively constant properties requiring minimal on-line measurement.

Operation of the robust reactor is at the cost of long batch time as well as drift in both polymer molecular weight and composition in the early stages of the batch. Therefore, it is important to improve reactor efficiency of quality monitoring and operation which will enhance product quality, production rates, safer operation, and subsequently improve profits. A dynamic model is developed to test the on-line optimization algorithm for the starved-feed free-radical copolymerization of butyl methacrylate and styrene (BMA/ STY) system, which reduces batch time while improving product uniformity. Three case studies are discussed to show the result of the optimization technique.

I. Description of System

Solution free-radical BMA/STY copolymerization was performed under starved-feed condition at 138˚C. Monomer is added to the reactor at a constant rate over 6 hours at different mass ratio (feed compositions) with tert-butyl peroxyacetate initiator fed at a constant mass ratio of 2.0 wt% relative to monomer feed. The process is illustrated in Figure 1.

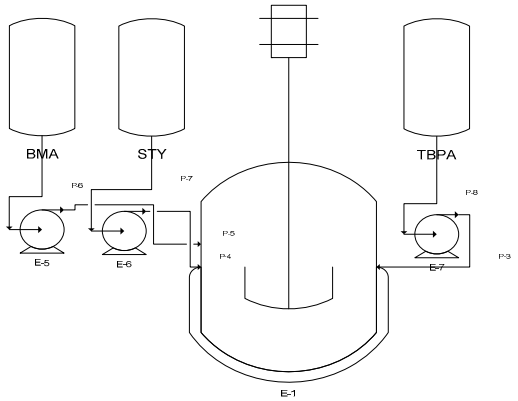

Figure 1: Schematic of semibatch reactor system. The flow rates of butyl methacrylate (BMA) and styrene (STY) monomers and tert-butyl peroxyacetate (TBPA) initiator can be independently manipulated.

The monomer and polymer compositions were shown [1] to be relatively uniform throughout the reaction in the semi-batch reactor as the free BMA and STY monomer levels were low for the whole experimentation.

II. Process Model

A full model [1] was developed for off-line optimization and product development of the present starved-feed feeding method containing a defined set of kinetic mechanisms for semi-batch high temperature BMA/ STY copolymerization. For this study, a mathematical model was formulated based on a reduced set of kinetic mechanisms embedded into the overall material balances in order to capture the basic process performance to design an efficient and robust system to control polymer quality. Methacrylate depropagation, styrene thermal initiation, and penultimate propagation kinetics were not incorporated in the mechanistic set.

Under standard assumptions such as perfect mixing, constant physical properties, quasi steady-state assumption (radical stationarity) and long chain hypothesis, mass balances on the initiator, solvent and monomers, and moment balances on the radical (live) and dead polymer chains yield the isothermal mathematical model for the semibatch system summarized below. The resulting set of differential equations describing the semibatch isothermal copolymerization is:

$$
\begin{aligned}
\frac{d(x_1(t))}{dt} &= u_1(t) - x_1(t)(k_{p_{AA}}\lambda_o^A(t) + k_{p_{BA}}\lambda_o^B(t)) \\
\frac{d(x_2(t))}{dt} &= u_2(t) - x_2(t)(k_{p_{BB}}\lambda_o^B(t) + k_{p_{AB}}\lambda_o^A(t)) \\
\frac{d(x_3(t))}{dt} &= u_3(t) - k_d x_3(t) \\
\frac{d(x_4(t))}{dt} &= x_1(t)(k_{p_{AA}}\lambda_o^A(t) + k_{p_{BA}}\lambda_o^B(t)) \\
\frac{d(x_5(t))}{dt} &= x_2(t)(k_{p_{BB}}\lambda_o^B(t) + k_{p_{AB}}\lambda_o^A(t)) \\
\frac{d(x_6(t))}{dt} &= V(t)(R_{\mu_0}(t))
\end{aligned}
\qquad (1)
$$

where $x_1(t)$ and $x_2(t)$ represent the total mass of unreacted BMA and STY in the reactor, while $x_3(t)$ is the mass of unreacted initiator. States $x_4(t)$ and $x_5(t)$ represent the mass of BMA and STY contained in the polymer chains, and the number of moles of polymer chains is represented by $x_6(t)$.

The reduced model derived in this work capture the essential dynamics of the full model and the experimental data [1]. The primary references for these coefficients and parameters are contained in the work of Li and Hutchinson [1]. Various quantities of interest can be calculated from the states. For the semibatch reactor, monomer conversion is defined as the mass of polymer in the reactor divided by the mass of monomer and polymer:

$$\chi_m(t) = \frac{x_4(t) + x_5(t)}{x_1(t) + x_4(t) + x_2(t) + x_5(t)}$$

Number-average molecular weight and copolymer composition (BMA mole fraction), denoted by M_n and F, are calculated as follows:

$$M_n(t) = \frac{x_4(t) + x_5(t)}{x_6(t)}, \quad F(t) = \frac{x_4(t)}{\overline{M}_A} \Big/ \left(\frac{x_4(t)}{\overline{M}_A} + \frac{x_5(t)}{\overline{M}_B} \right)$$

An objective of the starved-feed strategy is to keep these latter two quantities uniform throughout the course of the semibatch reaction, while maintaining high conversion in the reactor. Thus, the objective function is defined so as to minimize the batch time and maintain the copolymer molecular weight (M_n) and composition (F) at their targets values throughout the batch while also satisfying path and terminal constrains on the states and/or the controls.

III. Real-Time Optimization Mechanism

An optimization technique [2] is utilized to design a control structure that satisfies the specific objectives of the system under study discussed in the previous section. The feedback measurements are incorporated directly into the optimization procedure rather than into a low level tracking controller making it an online optimization instead of an online re-optimization, therefore eliminating the need for controller design and related difficulties. The technique used in this study is different from existing online optimization techniques ([3],[4],[5],[6]) as it involves minimal computational requirements, provides stable closed-loop performance and does not require knowledge of a nominal optimal solution.

The control problem undertaken in this study is to find the input trajectory that solves the dynamic optimization problem for some user defined cost function *J*. A dynamic optimization problem is formulated describing the feed flow rates parameters and the time interval lengths as decision or optimizing variables. For tracking purposes the objectives for M_n and F have been aggregated into a single scalar function while defining the batch time as a terminal objective function:

$$J = \int_0^{t_f} (\omega_1 (\frac{M_n(t)}{M_{sp}} - 1)^2 + \omega_2 (\frac{F(t)}{F_{sp}} - 1)^2) dt + \omega_3 t_f \qquad (2)$$

where J is the objective function to be minimized, and M_{sp} and F_{sp} are the target values for molecular weight and composition respectively. The set of weights to scale the objectives are defined by $\omega_1, \omega_2, \omega_3$. The optimization is subject to process dynamics (1) and the constraints described below.

A suitable means to limit potential heat release is to place constraints on unreacted monomer in the reactor. The monomer and initiator levels in the batch must not exceed certain maximum limits to meet safety constraints related to heat release. These constraints are described by:

$$0 \le x_k(t) \le x_k^{\max}, \; x_{k+3}(t) \ge 0 \quad k \in \{1,2,3\} \qquad (3)$$

Actuator limitations often dictate control constraints, whereas non-negativity of flow rates is a common input constraint.

$$0 \le u_k(t) \le u_k^{\max}, \quad k \in \{1,2,3\} \qquad (4)$$

Terminal constraints are commonly related to safety or productivity considerations. With regard to the latter, the desired mass of polymer at the batch end is specified as an endpoint constraint:

$$x_4(t_f) + x_5(t_f) = m_{pol}(t_f) \tag{5}$$

The control functions are parameterized in three distinct strategies. The first (Case 1) and simplest strategy considers using a single constant: $u_k(t) = u_k$ ($k = 1,2,3$) through the entire batch time horizon subject to a starved-feed operation. The corresponding control parameterization is given by:

$$u_1(t) = \theta_1,\ u_2(t) = \theta_2\theta_1,\ u_3(t) = \theta_3\theta_1 \tag{6}$$

The second parameterization (Case 2) considered in this work allows for exponential feeding in a starved-feed operation. This parameterization is written as follows:

$$u_1(t) = \theta_1 e^{\theta_2 t},\ u_2(t) = \theta_3 u_1(t),\ u_3(t) = \theta_4 u_1(t) \tag{7}$$

The final parameterization (Case 3) allows for independent exponential feeding strategy. The objective is to verify the cost of utilizing a starved-feed strategy in practice. This slightly more complex parameterization is given by:

$$u_1(t) = \theta_1 e^{\theta_2 t},\ u_2(t) = \theta_3 e^{\theta_4 t},\ u_3(t) = \theta_5 e^{\theta_6 t} \tag{8}$$

Note that eq.(8) can be reduced to either eqs.(7) or (6) for specific choices of the parameters $(\theta_1, \theta_2, \theta_3, \theta_4, \theta_5, \theta_6)$.

The objective of the optimization technique is to steer the system to the local optimum of the user-defined cost eq.(2) subject to a specific parameterization (*i.e.* from eqs. (6), (7) and (8)) while responding in real-time to changes in plant operation. The technique cannot be used to recover the actual optimal control but provides suboptimal control strategies and allows the adjustment of the parameters of the input parameterization in a way that provides continuous improvement with respect to the user-defined cost function. Constraint satisfaction is also satisfied.

The constrained problem is transformed to the minimization of the unconstrained cost:

$$J_{ip} = \int_{\tau}^{1} \left[t_f \left(\omega_1 \left(\frac{M_n(\sigma)}{M_{sp}} - 1 \right)^2 + \omega_2 \left(\frac{F(\sigma)}{F_{sp}} - 1 \right)^2 \right) - \mu_1 \sum_{j=1}^{z=m} \log(w_j + \varepsilon) \right] d\sigma + \omega_3 t_f + M (w_f)^2 \tag{9}$$

where the *m* path constraints w_j are given by:

$$w_k = -x_k - x_k^{\max} + \varepsilon,\ \ w_{k+3} = x_k + \varepsilon\ ,\ \ k = 1,2,3$$

control constraints by:

$$w_{k+6} = -u_k + u_k^{\max} + \varepsilon,\ w_{k+9} = u_k + \varepsilon\ ,\ \ k = 1,2,3$$

and end point constraints by:

$$w_f = x_4 + x_5 - m_{pol}(t_f)$$

Numerical values for the bounds of the path constraints are given with the cases studies. The integral part of the modified cost is considered as an additional state such that:

$$\dot{x}_7 = \frac{dx_7(\tau)}{d\tau} = t_f(\omega_1(\frac{M_n(\tau)}{M_{sp}} - 1)^2 + \omega_2(\frac{F(\tau)}{F_{sp}} - 1)^2) - \mu_1 \sum_{j=1}^{z=m} \log(w_j + \varepsilon) \qquad (10)$$

Finding a locally optimal solution can often be achieved through appropriate initial guesses to the optimizer and the use of realistic constraints. However, to find a feasible set of initial guesses is sometimes not a trivial task due to the interior feasible point method (barrier function) used. The barrier method requires that the initial guess of the solution to be strictly feasible. In addition, ill conditioning inherent to the nonlinearity of the reactor system may play a role in the sensitivity of the solution to initial conditions.

The constrained parameter set $\Omega = \{\theta \in \Re^N \mid w(x^p(t), \varphi(\theta, t)) \geq 0\}$ describes a convex subset of $\Re^N$. It is assumed that the parameters evolve on a compact subset γ of $\Re^N$, and that the cost functional $J : \Re^N \to \Re^N$ is convex and continuously differentiable on γ. The assumptions made up to this point guarantee a local optimization of the constrained problem exists and that the gradient can be used to achieve that minimization [2].

An interior point method with penalty function is used to include the constraint costs. The interior point method incorporating a log barrier function enforces the state and input constraints (essentially converting the constrained optimization problem into an unconstrained one) while the end-point constraints are incorporated through a terminal penalty function. In the remaining equations obvious notation has been omitted. Thus, let the path cost with barrier function be stated as follows:

$$L(x,u) = q(x,u) - \sum_{i=1}^{nc} \mu_1 \log(w_i(x,u) + \varepsilon) \qquad (11)$$

To emphasize that the optimization is based on the current conditions, the new cost functional with interior point method and penalty function is stated as:

$$J_{ip} = \int_t^{t_f} L(x^p(\tau), \varphi(\theta, \tau)) d\tau + M \parallel x^p(t_f) - x_f \parallel^2 \qquad (12)$$

where $\tau \in [t, t_f]$ is the integration variable and nc is the number of inequality constraints. The parameter $\mu_1 > 0$ is the barrier parameter for the logarithm term, $M > 0$ is the penalty term and $\varepsilon > 0$ is a constraint relaxation factor (back-off) that prevents the barrier term from singularity.

The formulation uses a gradient-based method for the solution of the dynamic optimization problems in real-time, with a straightforward diagonally scaled steepest descent parameter update law of the form:

$$\dot{\theta} = -\text{Proj}(\Gamma \nabla_\theta J_{ip}, \Omega_w) \qquad (13)$$

where $\Gamma > 0$ is the scaling matrix (referred as a gain matrix) to be defined later. To avoid divergence of the update law a projection algorithm is used. This guarantees that the parameters remain in a convex set $\Omega_w = \{\theta \in \Re^N \mid \parallel \theta \parallel \leq \eta\}$ for some $\eta > 0$ while assuring that the cost decreases until the optimal profile parameters are determined.

A Lyapunov-based method was used to show convergence to the local minimizers of a user-defined cost functional. The projection algorithm is given by:

$$\dot{\theta} = \begin{cases} \gamma, & \text{if } \| \theta \| < \eta \text{ or } (\|\theta\| = \eta \text{ and } \nabla P(\theta) \le 0) \\ \psi, & \text{otherwise} \end{cases}$$

where $\psi = \gamma - \gamma \frac{\nabla P(\theta) \nabla P(\theta)^T}{\| \nabla P(\theta) \|^2}$, γ is a compact subset of $\Re^n$ where the parameters are assumed to evolve, $P(\theta) = \theta^T \theta - \eta$, θ is the vector of input parameters and η is chosen such that $\| \theta \| \le \eta$.

IV. Case Studies

Cases 1-3 illustrate the optimization of the BMA/STY system relative to the conventional starved feed strategy for the 50:50 BMA: STY mass ratio. Cases 1 to 3 follow experimental initial conditions (monomer and initiator feed rates) used in the experimental study of [1] and summarized in Table 1. In Table 1, m_{TBPA}^{fed}, m_{BMA}^{fed}, and m_{STY}^{fed} represent the total mass of initiator, BMA and STY fed to the reactor to the final batch time of t_f. The mass of polymer produced at the final batch time is $m_{pol}(t_f)$, taken as the terminal (end-point) constraint in the optimization routine and set so that the final weight fraction of polymer in solution is 0.7 at the end of the batch.

Table 1: Conventional starved feed strategey used in [1]

Results	50:50 BMA:STY (wt ratio)	75:25 BMA STY (wt ratio)
m_{TBPA}^{fed}, Kg	9.7E-03	9.7E-03
m_{BMA}^{fed}, Kg	2.46E-01	3.6E-01
m_{STY}^{fed}, Kg,	2.46E-01	1.23E-01
t_f, min	360	360
$m_{pol}(t_f)$	0.474	0.483

For all three cases, the target values of F_A and M_n (g/mol) are 0.43 and 11 respectively. The constraints for the states and input variables are set to: $x_1(t) \in [0, 0.02]$, $x_2(t) \in [0, 0.02]$, $x_3(t) \in [0, 5.0 \times 10^{-4}]$ and $u_i(t) \in [0, 0.01]$, $i = 1, 2, 3$. The algorithm parameters for all three cases are as follows. The adaptive gain (k) in the steepest descent law used by the algorithm is 0.0001. The end constraint parameter M is set to 10^8. This large value ensures that endpoint values are strictly enforced. The barrier function parameters, μ and ε, are set to 0.1 and 10^{-7}, respectively. The initial conditions for the system are $x_1(0) = x_2(0) = x_3(0) = x_4(0) = x_5(0) = x_6(0) = 0$.

Table 2 Performance metrics for the three cases.

Case	$m_{pol}(t_f)$ (kg)	t_f (sec)	$J_{ip}(t_f)$
1	0.47386	15335	1.8988×10^5
2	0.47383	15479	1.8565×10^5
3	0.47383	15234	1.7706×10^5

As summarized in Table 2, the more general parameterization from Case 3 provides some improvements in performance over the simpler Cases 1 and 2. All cases provide a significant improvement over the experimental batch time of 21600 seconds. In all three cases, the optimization routine successfully implements a feasible locally optimal strategy for the given parameterization that 1) improves the nominal performance of the fed-batch system and 2) enforces constraint satisfaction in the monomer feed. Figure 2 compares the results obtained using the real-time optimization technique for Case 3 to the nominal results from the feed-rate used in [1] that resulted in a batch time of 21600 seconds. These curves are labeled "simulation" on the plots.

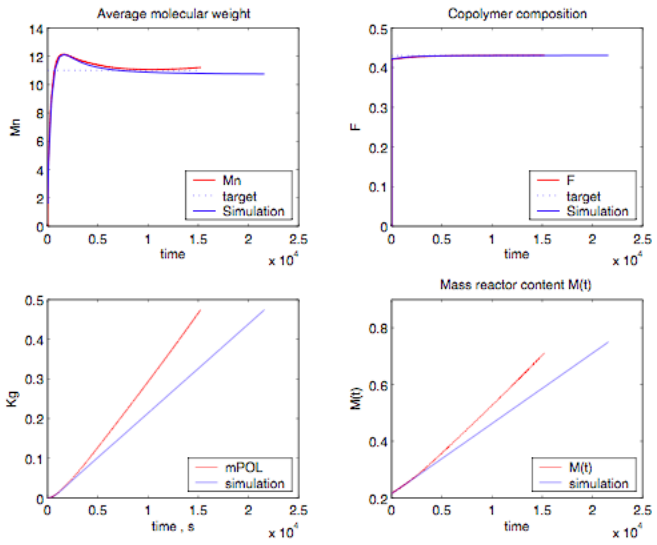

Figure 2: Performance of the real-time optimization control system and the nominal fed-batch strategy.

Figure 3 shows the state trajectories for Case 3. It can be seen that the real-time optimizing controller pushes $x_3(t)$ to its upper limit. Relaxation of this constraint should result in further reduction in batch time. Figure 4 shows the corresponding input trajectories. As expected, the effect of the constraint in $x_3(t)$ is shown in the trajectory for $u_3(t)$. On average the real-time optimization routine requires 1 to 10 msec of computation for every second of operation. The corresponding controller is therefore viable for implementation.

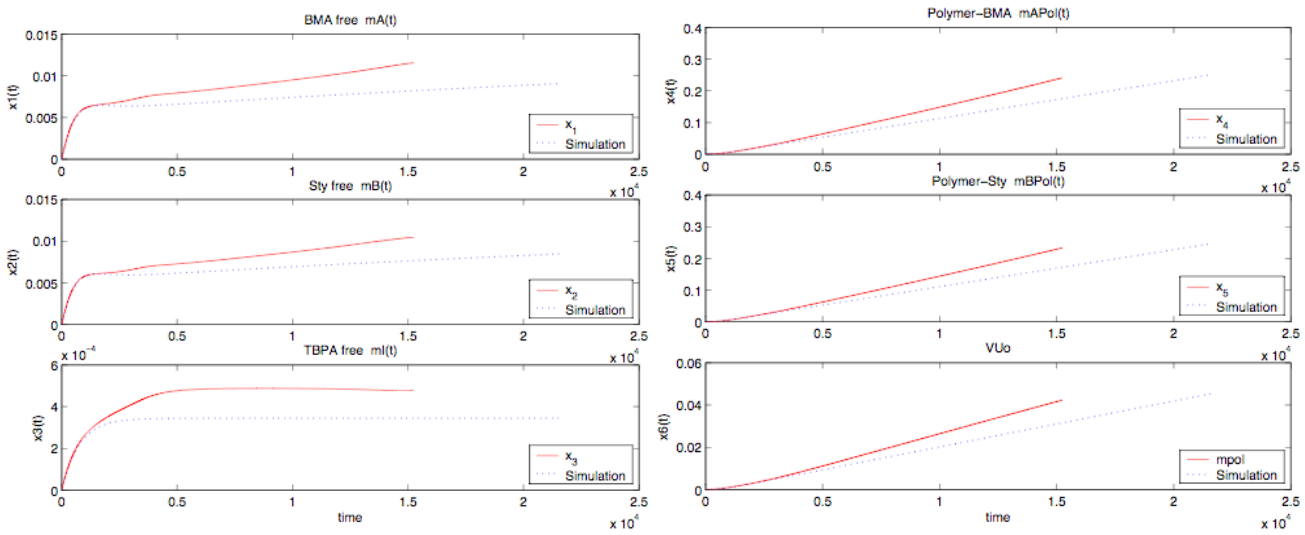

Figure 3: State trajectories for Case 3. The nominal simulation based on the experimental conditions in [1] are also shown.

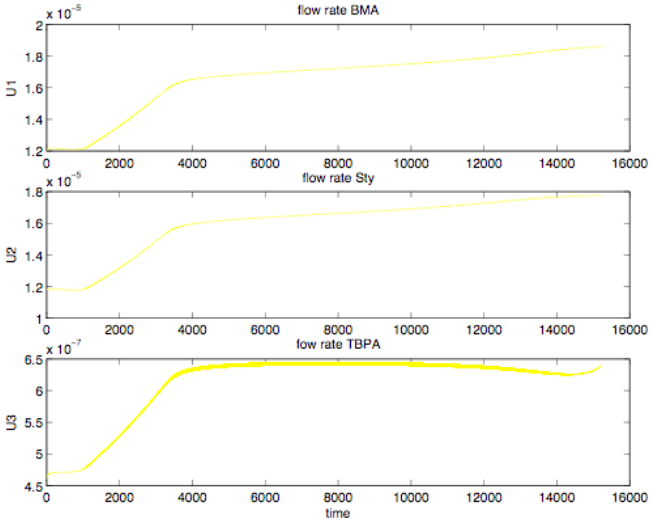

Figure 4: Input trajectory for Case 3.

V. Conclusions

Considerable improvements in polymer quality (less drift in molecular weight and copolymer composition) and productivity (batch time reduction) can be obtained while satisfying the constraints imposed to the system. Moreover, this novel technique and the use of a reduced order model result in low computational effort that can be further exploited through more complex input parameterization and/or the use of a more complex model to improve the accuracy of the model predictions. The actual implementation will be the main focus of further experimental study. Ongoing research in this area has demonstrated the promise that a viable estimation routine can be developed and implemented.

Acknowledgement

The authors acknowledge the support of the Natural Sciences and Engineering Research Council of Canada and E.I. du Pont de Nemours and Co.

References

[1] Li, D. and R.A. Hutchinson, *High temperature semibatch free radical copolymerization of butyl methacrylate and styrene.* Macromolecular Symposium, 2006. **243**: p. 24-34.

[2] Peters, N., D. Dehaan and M. Guay, *Real-Time Dynamic Optimization of Nonlinear Batch Systems.* Journal of Process Control, 2007. **17**(3): p. 261-271.

[3] Abel, O.and W. Marquardt, *Scenario-integrated on-line optimization of batch reactors.* Journal of Process Control, 2003. **13**: p. 703-715.

[4] Chen, H. and. F. Allgöwer,, *Nonlinear model predictive control schemes with guaranteed stability*, in *Nonlinear Model Based Process Control*. 1998, Kluwer: Dordrecht, The Netherlands. p. 465-494.

[5] Mayne, D.Q., Rawlings, J.B., Rao, C.V., Scokaert, P., *Constrained model predictive control: stability and optimality.* Automatica, 2000. **36**(6): p. 789-814.

[6] Richards, J.R. and J.P.Congalidis, *Measurement and control of polymerization reactors.* Computers and Chemical Engineering, 2006. **30**: p. 1447-1463.